

IBM Research Report

Photoelectron Spectroscopy of Individual Si Nanowires

Richard Haight, George Sirinakis, Mark Reuter

IBM Research Division

Thomas J. Watson Research Center

P.O. Box 218

Yorktown Heights, NY 10598



Research Division

Almaden - Austin - Beijing - Haifa - India - T. J. Watson - Tokyo - Zurich

Photoelectron Spectroscopy of Individual Si Nanowires
Richard Haight*, George Sirinakis and Mark Reuter
IBM T.J. Watson Research Center
PO Box 218
Yorktown Hts., N.Y. 10598

ABSTRACT

We describe an experiment designed to investigate the electronic structure of individual nanowires of Si. Laser generated 150 femtosecond pulses of photons with a wavelength of 200 nm (6.2 eV) were focused onto an individual Si nanowire. Photoelectrons emitted from the wire were collected and energy analyzed by an electrostatic spectrometer with 20 meV resolution. Si wires, grown across gaps on a lithographically patterned substrate, exhibited diameters that varied between 20 and 400nm depending on growth conditions. In these experiments we have observed strong polarization dependent electron emission consistent with Mie theory. We have measured the location of the Fermi level within the intrinsic Si wire band gap, the work functions of individual hydrogen terminated wires, which are compared with those of Ge nanowires, and observed polarization dependent spectral features. Variations in spectral features from wire-to-wire are suggested to derive from size dependent growth directions and faceting.

*To Whom Correspondence Should Be Addressed, Email: rahaight@us.ibm.com

Semiconductor nanowires (NW) are of particular technological importance owing to the substantial existing infrastructure devoted to Si electronics, but there is also strong fundamental interest associated with their low- dimensional character. Since control on the NW size can be achieved by a number of growth mechanisms including the widely used vapor-liquid-solid (VLS) [1] process, the potential to study individual wires and the corresponding properties of electrons confined in two dimensions is particularly alluring. While the study of the structure of an individual NW is amenable to a technique such as transmission electron microscopy, spectroscopic information on their electronic states has for the most part been acquired from ensembles of NWs of various diameters and lengths; the resultant averaging masks the detailed fundamental electronic structure of individual NWs[2].

In this paper we describe a novel application of photoelectron spectroscopy designed to isolate and study individual Si NWs. Wires with diameters ranging from ~20 nm to 400 nm have been isolated and valence band photoelectron spectra have been recorded. With this approach we have been able to study surface and bulk electronic properties as a function of wire diameter. We have located the wire Fermi level within the NW band gap for intrinsic Si NWs. We have also studied the photoelectron emission intensity as a function of the polarization of the light incident on the NWs and compared this with Mie theory, all of which will be described in this paper.

Photoelectron spectroscopy is a powerful tool to study the electronic structure of NWs, but its application introduces a unique set of challenges since light with energies $> 5\text{eV}/\text{photon}$ must be used in order to liberate electrons from the Si wire. In this experiment, 150 femtosecond pulses of 200 nm (6.2 eV) light are generated at a 250 kHz repetition rate from a regeneratively amplified Ti:sapphire laser operating at a fundamental wavelength of 800 nm. (Fig. 1). The 800 nm light is frequency quadrupled in three different beta-barium borate crystals to produce the 6.2 eV photons for photoemission. Since the work function of Si is below 5 eV, the top 1-2 eV of the valence bands of these wires can be accessed via the absorption of a single photon.

Si wires are grown using the VLS process which has been described in detail in the literature¹. In our experiment the NWs are grown on Si wafers lithographically patterned with 30-40 micron wide slots, etched completely through the wafer, and dressed with alphanumeric markers for location of the wires. By proper control of the growth process, individual NWs were typically separated by at least several microns along the length of the slot. A collimated beam of 200 nm light is directed along the optical axis of a Swartzchild reflective objective (0.5 NA), resident in a vacuum chamber, and focused on an individual wire. Electrons are emitted from the opposite side of the wire and emerge from a rectangular region defined by the focal spot diameter (~ 1 micron) and the NW diameter. They are subsequently energy analyzed by an electrostatic detector with 20 meV resolution.

The NWs are positioned under the objective using a two-axis piezoelectrically driven stage. Although not easily resolved with the imaging system, NWs are observable from scatter of

the 248 nm imaging light as well as the much brighter and distinct scattered light observed as the 200 nm photoemission pulse is scanned across the NW (Fig. 1) .

Since the NWs we are interested in studying are in the range of tens to hundreds of nanometers in diameter, photoelectron spectroscopy with low energy photons is particularly advantageous. In Si, the light intensity drops to its e^{-2} value ~ 10 nm from the surface[3]. For electrons with 1-2 eV kinetic energy, the mean free path within Si is > 100 nm[4], so that even for thicker wires, photoexcited electrons can transit through the NW to reach the electron analyzer. In this manner our spectroscopic setup and geometry permits the study of surface as well as bulk electronic states. Changes in the photoemission intensity were studied as a function of the input light polarization, facilitated by rotating a half-wave-plate external to the vacuum system. Care was taken to insure the same light flux on the NW for all polarizations. The Fermi level, critically important to the study of the location of the NW valence band edge was determined by deposition of Au in contact with the sample. A -15 V bias was applied to the NWs to permit observation of the entire NW spectrum; as a result work functions of the NWs and deposited metals could be measured.

Numerous NWs of various diameters, resulting from either changes in the VLS growth conditions or from intentional oxidative thinning[5], were identified and measured with scanning electron microscopy (SEM). Active thinning of the NWs was achieved by furnace annealing of the sample in an oxygen ambient which formed an SiO_2 shell that was subsequently removed in a hydrofluoric (HF) acid vapor. All samples were exposed to HF

vapor to remove residual SiO₂ and to hydrogen terminate the surfaces of the NWs before measurement.

Photoelectron spectroscopy is highly sensitive to surface and bulk electronic structure; this structure can then, in principle, be correlated with the NW crystallographic orientation. The wide array of NWs we studied resulted in spectra that displayed a number of features, some of which varied from wire to wire and some that were consistently reproduced. Figure 2 shows spectra collected from a 35 nm Si NW with light polarized parallel (black) to the wire axis and separately perpendicular (red) to the wire axis. In this figure, the Fermi level (E_F) is located at 0 eV binding energy while the NW valence edge is at 0.65 eV. Hence the Fermi level is near the middle of the Si NW band gap, consistent with the undoped nature of the NWs. This location for E_F was observed for all of the NWs we studied. We note that for NWs with diameters >10 nm no significant quantum confinement induced band gap changes are expected[6].

For the NWs we studied, the electron emission threshold, E_T , which also determines the work function Φ via the equation $\Phi=6.2-E_T$, varied within an energetic span of ± 0.2 eV centered about 2.1 eV. For the particular wire in Fig. 2, the threshold was located at 2.08 eV and the corresponding value for the work function, $\Phi =4.12$ eV. A useful comparison of the details of the Si NW spectrum can be made with a spectrum collected from a Ge NW (Fig. 3 bottom spectrum). We note that the Ge NW valence band edge is found at 0.3 eV and the threshold energy, $E_T=1.77$ eV. Since the Ge NWs were grown undoped we again expect, and find, the

Fermi level to be near the middle of the Ge band gap. In addition $\Phi = 4.43$ eV for this NW, which is 300 meV larger than for the Si NW discussed above.

The variability we observe in E_T and spectral features is displayed in Fig. 3 where three different Si NWs of roughly the same diameter are plotted. A spectrum from a Ge NW is shown as well. We believe this variability is due to both NW faceting and differences in growth direction. In our experiment, since electrons emerge from the back surface of the wire a variety of facet orientations are possible. As discussed by Wu[7], wires exhibit diameter dependent growth directions ranging from the $\langle 110 \rangle$ to the $\langle 112 \rangle$ and $\langle 111 \rangle$ for increasing wire diameters. In addition faceting[6] and the appearance of sawtooth structures on the NW sidewalls[8] at larger diameters provide even greater variation where it was shown via UHV transmission electron microscopy that $\langle 111 \rangle$ oriented wires display predominantly (112) facets. In order to quantify this facet dependence, we measured Φ for H-terminated planar Si surfaces in a separate higher energy (26.35 eV photons) photoemission spectroscopy system, described elsewhere[9], and found $\Phi = 4.48$ eV, 4.42 eV and 4.56 eV for the H-terminated (110), (111) and (100) planar Si surfaces respectively. For the H-terminated Ge (111) surface we found $\Phi = 4.84$ eV, which is 300-400 meV larger than that for the planar H:Si surfaces. While not providing a direct correlation with specific NW facets, these measurements suggest that the range of Φ 's we observe is consistent with NW faceting. That the NW Φ 's are smaller than the planar H:Si and H:Ge values is not unexpected since edges associated with the faceted surfaces are expected to reduce Φ in a manner similar to that found for stepped or roughened surfaces[10]. Our SEM studies revealed facets in only a few isolated

cases on large diameter NWs; a significant challenge that remains is to directly correlate facet orientations with electronic structure of individual NWs.

In addition to the energetics described above we also observed a striking difference in the intensity and shape of the spectra when light was aligned parallel (black curve) or perpendicular (red curve) to the axis of the wire (Fig. 2). As we will describe below, this difference is a result of the polarization dependent optical absorption and scattering properties of the wire at 6.2 eV as described by Mie theory. Furthermore, it is well known in photoelectron spectroscopy that the transition matrix elements coupling occupied electronic bands to free-electron final states are polarization dependent; we ascribe the substantial changes in the 1.9 eV emission feature in Fig. 2 to such matrix element effects[11,12, 13] .

Aside from polarization dependent band structure effects, large diameter NWs displayed overall greater spectral intensity when the 6.2 eV light was polarized perpendicular to the NW axis, while this effect was inverted for small diameter NWs, i.e. greater spectral intensity was observed for light polarized parallel to the NW axis. To quantify this effect more thoroughly, we studied the polarization dependence as a function of NW diameter by oxidative thinning as described above. The results are shown in Fig. 4 where the polarization

anisotropy $\rho = \frac{I_{//} - I_{\perp}}{I_{//} + I_{\perp}}$ is plotted as a function of NW diameter and $I_{//}$ and I_{\perp} are the

spectral intensities collected with parallel or perpendicularly polarized light. In addition to repeatedly oxidizing and etching of an individual wire to achieve thinning (circles in Fig.4) we also plot as-grown wires (squares) with a variety of diameters to insure that systematic errors associated with oxide etching did not affect the results. The insets in Fig. 4 show

typical spectra for larger and smaller diameter wires. We observed negative ρ values for wires with diameters > 100 nm and positive ρ values for wire diameters < 100 nm. This striking inversion in the polarization dependence agrees qualitatively with calculations derived from Mie theory (solid curve) for 200 nm light scattering from a dielectric cylinder (Si).

Previous studies of the interactions of polarized light with NWs have been discussed within the context of the Rayleigh approximation[14,15] where electrostatics are invoked to calculate the polarizability of the NW with charges induced by the incident light on the NW surface. These charges screen the \mathbf{E} field of the incident light resulting in a decrease of the electric field inside the NW. Due to the one dimensional character of the NW this screening is stronger when the light is polarized perpendicular to the axis than when it is parallel. Hence absorption is preferentially enhanced when light is polarized parallel to the wire axis. The underlying assumption is that the NW is significantly smaller than the wavelength of the light, hence the \mathbf{E} field is approximately uniform over the region occupied by the NW at any instant. Additionally, the approximation requires that the absorption coefficient of the NW is small. However at a photon energy of 6.2 eV, Si is a strong absorber, with a bulk absorption coefficient[3] of ~ 2.9 which limits the validity of Rayleigh approximation even for Si NWs below 20 nm. To better understand the polarization dependence we applied Mie theory corresponding to the solution of the Maxwell equation's in a cylindrical coordinate system with appropriate boundary conditions at the surface of the cylinder[16]. In this manner, the extinction (Q_{ext}), scattering (Q_{sca}), and absorption ($Q_{abs} = Q_{ext} - Q_{sca}$) efficiencies are

expressed as a series of cylindrical harmonics. The solid curve shown in Fig. 4 is a result of this analysis.

Good qualitative agreement was obtained between theory and experimental data. Photoemission spectra of NWs with diameters smaller than the incident wavelength, but still comparable to the penetration depth, exhibit a polarization-dependent behavior which can be qualitatively understood within Rayleigh approximation. These NWs exhibit enhanced optical absorption for light polarized parallel to their axis. However, as the NW diameter is increased the Rayleigh approximation breaks down as higher order multipole terms become increasingly important, and the polarization anisotropy is inverted. The inversion point is theoretically predicted at a nanowire diameter of ~ 50 nm while experimentally it is found at ~ 100 nm.

Mie theory assumes an abrupt boundary between the dielectric (NW) and the surrounding medium and does not account for the detailed electronic structure and deviation of the NW from cylindrical (faceting). In addition, the NW surface is hydrogen-terminated. Given these sources of non-ideality, the agreement between calculation and our data to within a factor of 2 is quite reasonable and provides a framework for understanding the interaction of short wavelength light with semiconductor NWs.

In conclusion, we have described a new experiment to study the electronic structure of individual nanowires of Si and Ge with photoelectron spectroscopy. We anticipate that this

approach will be applicable to a wide range of systems such as carbon nanotubes, nanowire heterostructures, doped wires and more.

Acknowledgements: The authors would like to acknowledge the assistance of Carlos Aguilar and Martin O'Boyle in the initial construction of the experiment and Ranjani Sirdeshmukh for fabrication of the patterned Si substrates used for nanowire growth.

References

-
- ¹ R.S. Wagner and W.C. Ellis, *Appl. Phys. Lett.*, 4, 89 (1964); R.S. Wagner, in “Whisker Technology”, ed. By A.P. Levitt (Wiley Interscience, N.Y. 1970)
- ² Y.F. Zhang, L.S. Liao, W.H. Chan, S.T. Lee, R. Sammynaiken, T.K. Sham, *Phys. Rev. B*, 61, 8298 (2000)
- ³ D.E. Aspnes, A.A. Studna, *Phys. Rev. B*, 27, 985 (1983)
- ⁴ M.P. Seah, W.A. Dench, *Surf. Int. Anal.*, 1, 2 (1979)
- ⁵ D. Shir, B.Z. Liu, A.M. Mohammad, K.K. Lew, S.E. Mohny, *J. Vac. Sci. Technol. B* 24, 1333 (2006)
- ⁶ D.D.D. Ma, C.S. Lee, F.C. Au, S.Y. Tong, S.T. Lee, *Science*, 299, 1874 (2003)
- ⁷ Y. Wu, Y. Cui, L. Huynh, C.J. Barrelet, D.C. Bell, C.M. Lieber, *Nano Lett.* 4, 433 (2004)
- ⁸ F.M. Ross, J. Tersoff, M.C. Reuter, *Phys. Rev. Lett.*, 95, 146104-1 (2005)

⁹ D. Lim, R. Haight, M. Copel, E. Cartier, *Appl. Phys. Lett.* 87, 72902-1 (2005)

¹⁰ K. Besocke, B. Krahl-Urban, H. Wagner, *Surf. Sci.*, 68, 39 (1977)

¹¹ R.I.G. Uhrberg, G.V. Hansson, U.O. Karlsson, J.M. Nicholls, P.E.S. Persson, S.A. Flodstrom, R. Engelhardt, E.E. Koch, *Phys. Rev. B* 31, 3795 (1985)

¹² L.S.O. Johansson, P.E.S. Persson, U.O. Karlsson, R.I.G. Uhrberg, *Phys. Rev. B* 42, 8991 (1990)

¹³ W. Eberhardt, F.J. Himpsel, *Phys. Rev. B* 21, 5572, (1980)

¹⁴ M.Y. Sfeir, F. Wang, L. Huang, C-C. Chuang, J. Hone, S.P. O'Brien, T.F. Heinz, L.E. Brus, *Science*, 306, 1540 (2004)

¹⁵ J. Wang, M.S. Gudiksen, X. Duan, Y. Cui, C.M. Lieber, *Science*, 293, 1455, (2001)

¹⁶ C. Bohren, D.R. Huffman, "Absorption and Scattering of Light by Small Particles" (Wiley) 1983

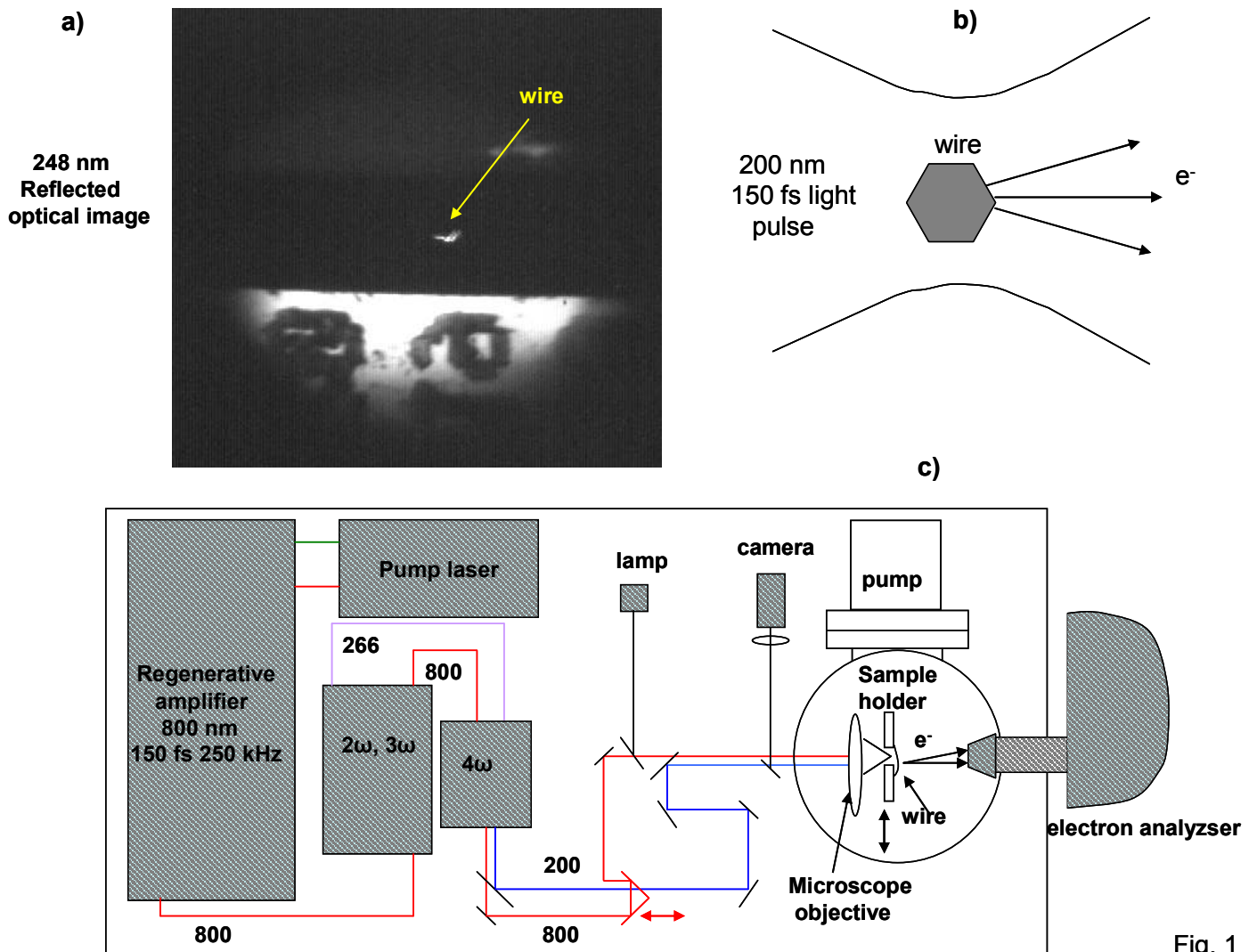


Fig. 1

Fig. 1
 a) Reflected light (248nm) image of a Si NW showing the edge of the 40 μ slot with numerical fiducial. The bright spot in the middle of the gap derives from 200 nm light scattered from the wire traversing the slot. b) Schematic diagram showing the 200 nm light pulse focused on the wire, shown in cross-section. c) Schematic of the experimental

setup. While not used in this experiment, the 800 nm light pulses are available for pump/probe experiments.

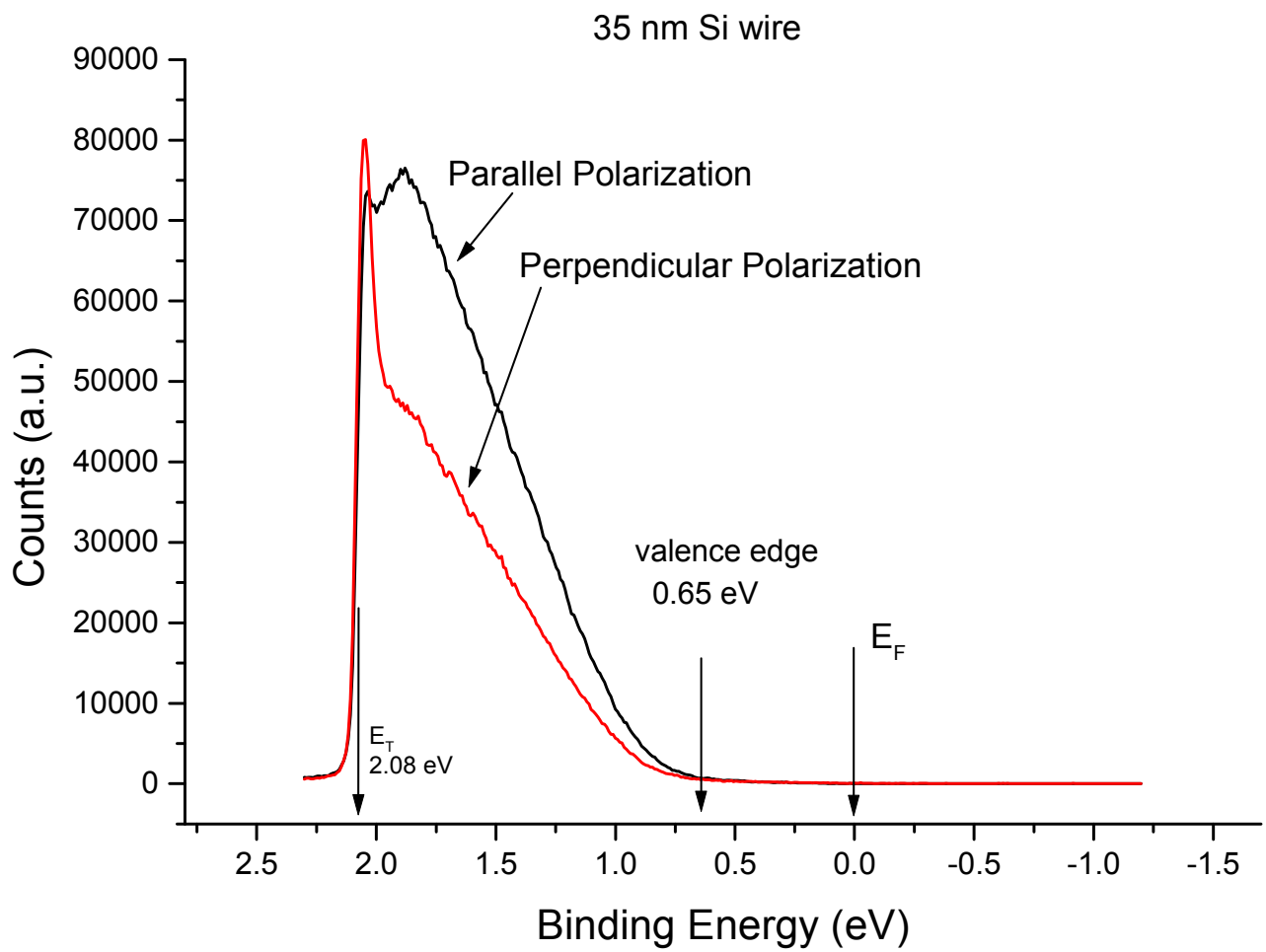


Fig. 2

Photoelectron spectra showing the emitted electron intensity as a function of binding energy for a 35 nm Si NW excited with 6.2 eV photons polarized parallel (black) and perpendicular (red) to the long axis of the NW. Arrows identify the Fermi level, E_F , valence band edge and electron emission threshold, E_T .

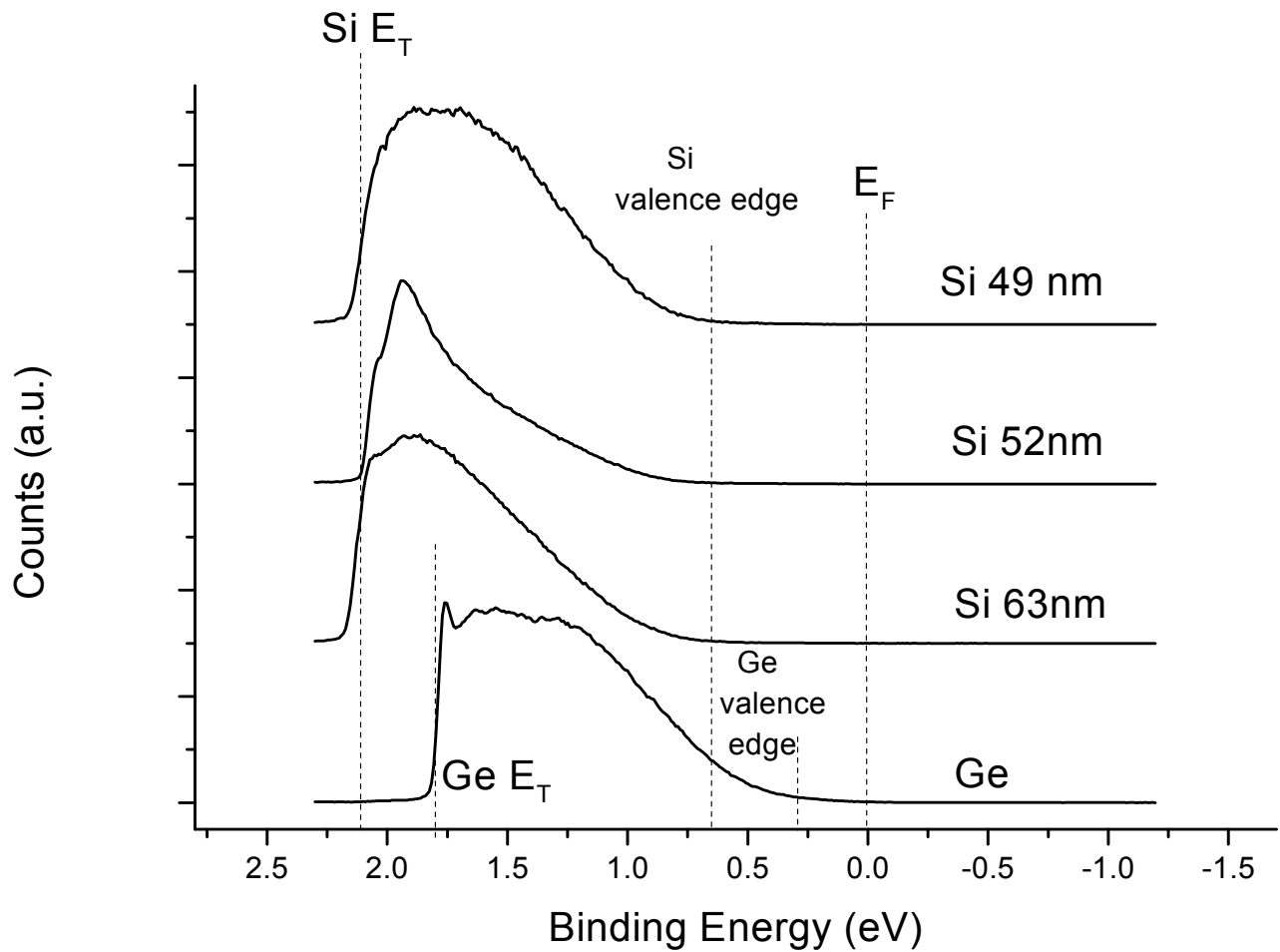


Fig. 3

Comparison of three different Si NW spectra with that collected from a Ge NW. For the Si (Ge) NWs, the electron emission threshold is at ~ 2.1 eV (1.77 eV) and the valence band edge is at 0.65 eV (0.3 eV).

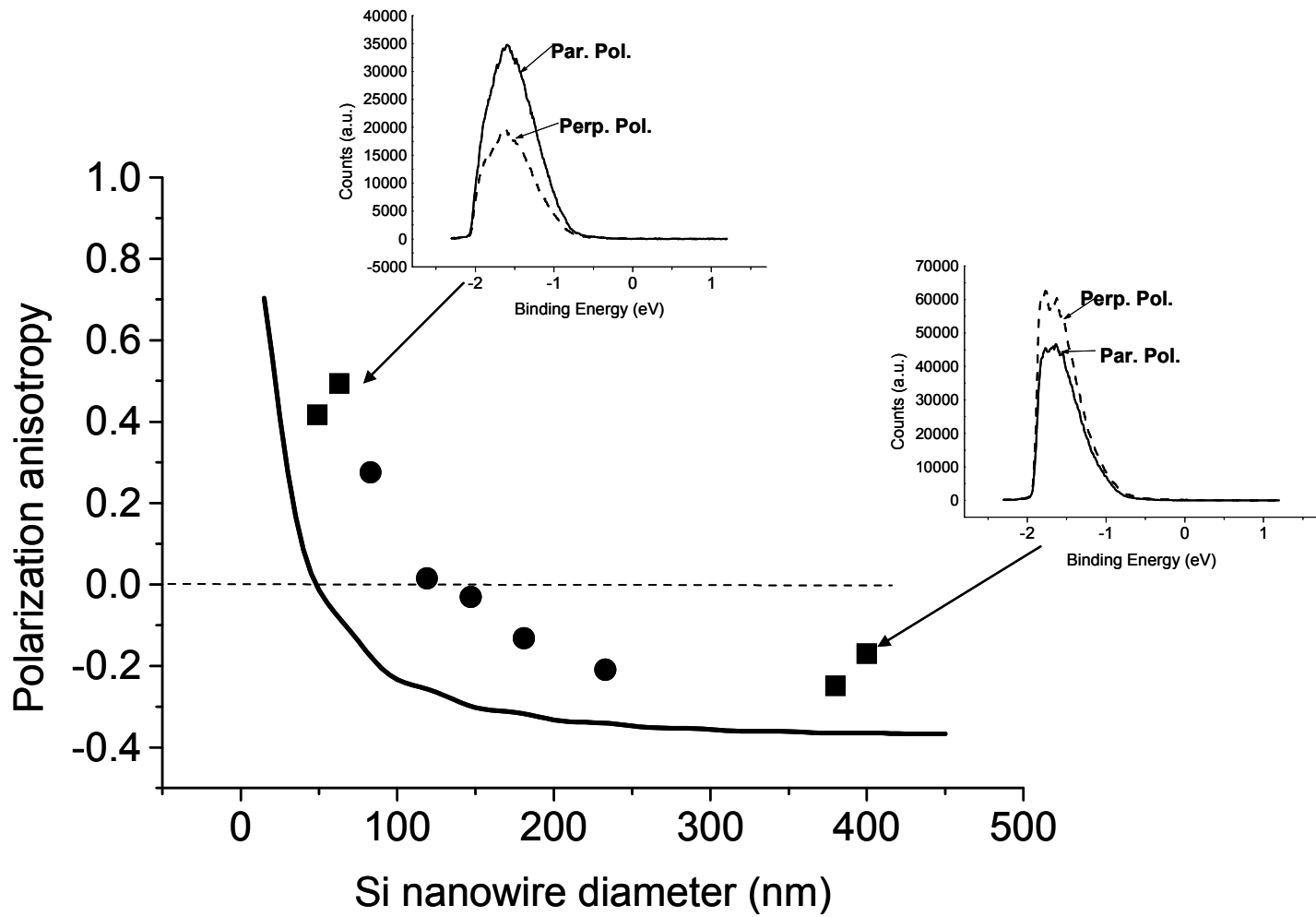


Fig. 4

Fig. 4

Plot of the polarization anisotropy, ρ , of a Si NW thinned by repeated oxidation and etching in HF vapor (circles) and as-grown NWs (circles). Insets display representative spectra for a large diameter Si NW and a small diameter Si NW. For the large NWs spectra collected with light polarized perpendicular to the NW axis are more intense, while for small diameter NWs the opposite is true.